Science of the Total Environment 1027 (2026) 181707

Contents lists available at ScienceDirect

Science of the Total Environment

journal homepage: www.elsevier.com/locate/scitotenv

The evaluation to combined toxic effects of polypropylene microplastics and benzo[*a*]pyrene on macrophage cells

Ye-xuan Zhang [a,1], Rui Hou [a,1], Si-si Chen [a], Xue-wen Guo [a], Hong-juan Chen [b], Li Mao [c], Wei-juan Zheng [b], Hong-zhen Lian [a,*]

[a] State Key Laboratory of Analytical Chemistry for Life Science, School of Chemistry & Chemical Engineering and Center of Materials Analysis, Nanjing University, Nanjing, 210023, China
[b] State Key Laboratory of Pharmaceutical Biotechnology, School of Life Science, Nanjing University, Nanjing, 210023, China
[c] Ministry of Education (MOE) Key Laboratory of Modern Toxicology, School of Public Health, Nanjing Medical University, Nanjing, 211166, China

HIGHLIGHTS

- Combined exposure of PP MPs and BaP causes enhanced toxicity compared to BaP alone.
- Co-stimulation of PP MPs and BaP to RAW264.7 cells causes elevated oxidative stress.
- Toxicoproteomics reveals that the co-exposure triggers intense inflammatory response.

GRAPHICAL ABSTRACT

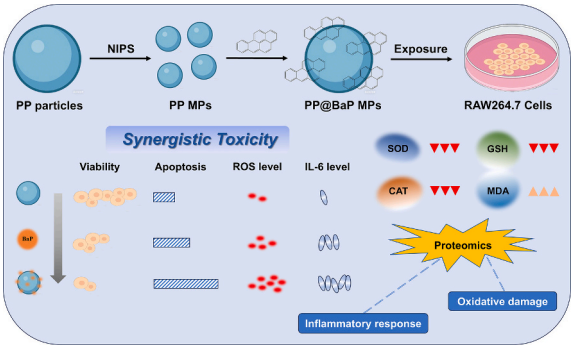

ARTICLE INFO

Keywords:
Polypropylene microplastic
Benzo[*a*]pyrene
RAW264.7 cells
Combined cytotoxicity
Proteomics

ABSTRACT

Microplastics (MPs) pollution has emerged as a significant concern for human health, and their toxicological mechanisms help to better understand their potential risks. Previous studies paid main attention on the toxicity of MPs themselves, but in recent years, there has been growing awareness of their combined effects with other environmental pollutants. This study investigated the toxic effects of polypropylene microplastics (PP MPs) prepared via nonsolvent induced phase separation method in conjunction with benzo[*a*]pyrene (BaP) stimulation in vitro to macrophagocytes based on toxicoproteomics. We observed that PP MPs alone exhibited no obvious toxicity to the cells at concentrations of 50–150 μg/mL, while individual BaP induced significant cytotoxicity. Moreover, the combined exposure of PP MPs and BaP caused enhanced toxicity compared to BaP alone, where their combined exposure significantly suppressed the proliferation of RAW264.7 cells, exacerbated cell membrane damage, and increased apoptosis, resulting in substantial cellular toxicity. The possible toxic mechanisms were explored by measuring oxidative stress levels. It was found that co-exposure to PP MPs and BaP markedly inhibited superoxide dismutase (SOD) and catalase activities (CAT), reduced glutathione (GSH) level, elevated

* Corresponding author at: State Key Laboratory of Analytical Chemistry for Life Science, School of Chemistry & Chemical Engineering and Center of Materials Analysis, Nanjing University, 163 Xianlin Avenue, Nanjing, 210023, China.
E-mail address: hzlian@nju.edu.cn (H.-z. Lian).
[1] These authors contributed equally to this work.

https://doi.org/10.1016/j.scitotenv.2026.181707
Received 16 October 2025; Received in revised form 10 February 2026; Accepted 16 March 2026
Available online 19 March 2026

malondialdehyde (MDA) level, and increased intracellular reactive oxygen species (ROS) level compared to individual BaP exposure. Furthermore, proteomic analysis suggested that combined stimulation could lead to more serious oxidative damage, and further trigger intense inflammatory responses, validated by significant alterations in SOD, CAT, GSH, MDA, ROS, and IL-6. Therefore, this study provides new insights into assessing the risks associated with combined exposure to MPs and polycyclic aromatic hydrocarbons.

1. Introduction

With the development of modern industry, increasing plastic pollution has led to an increased risk of exposure to microplastics (MPs) (Feng et al., 2023; Hirt and Body-Malapel, 2020; Liu et al., 2024; Zhong et al., 2023). Typically, plastic particles ranging in size from 5 mm to 100 nm are defined as MPs (Kershaw and Rochman, 2016; Xia et al., 2023). Recently, MPs have also been defined as particles ranging from 5 mm to 1 μm in size, with particles smaller than 1 μm being categorized as nanoplastics (NPs) (Dang et al., 2022; Hartmann et al., 2019). MPs can be classified into primary MPs and secondary MPs based on their origins (Yu et al., 2023). Primary MPs are mainly pre-production pellets used in the manufacturing of plastic products, as well as microbeads used in industrial applications or as abrasives in personal care products. Secondary MPs arise from the fragmentation and breakdown of larger plastic items through physical, chemical and biological processes. These can form during the use of various plastic products, such as microfibers shed from clothing during washing or tire wear particles, or they can form after the release of larger plastic items into the environment, where they break down due to environmental factors (Gewert et al., 2015). MPs can be found in many kinds of environments, from soil (Li et al., 2018) to aquatic systems like oceans, rivers, and swamps (Prata et al., 2019), as well as in the digestive tracts of various animals (Lechner and Ramler, 2015). Some studies have pointed out that MPs could cause severe cell damage, such as increased intracellular levels of reactive oxygen species (ROS) (Xia et al., 2007), exacerbation of cellular membrane damage (Salimi et al., 2022), occurrence of inflammatory responses (Palaniappan et al., 2021), and more significant DNA damage (Çobanoğlu et al., 2021).

The risk posed by MPs is significantly compounded by their ability to act as carriers for other pollutants. The large specific surface area and hydrophobic nature of MPs make them readily interact with hydrophobic organic pollutants like polycyclic aromatic hydrocarbons (PAHs) during environmental transport, forming MPs-pollutant complexes for mutual dissemination (Bhagat et al., 2021). Most PAHs are toxic, mutagenic, and carcinogenic, causing harm to human respiratory, nervous, liver, and kidney organs. They are recognized as the primary organic pollutants affecting human health (Kongpran et al., 2021). Benzo[*a*]pyrene (BaP), serving as a toxicity indicator for PAHs, is one of the most extensively studied substances [IARC, 2010]. Goswami et al. (2023) detected 61 target compounds in MPs from the coastal environments of Sri Lanka and Japan, with total PAHs concentrations reaching 16,300 and 1770 ng/g plastic, respectively. This co-exposure leads to interactive toxic effects. For instance, Xu et al. (2020) indicated that the *co*-exposure of polystyrene (PS) MPs and BaP influenced inflammation in zebrafish, as well as HBE and HBSMC cells, while other studies reported synergistic or antagonistic effects with different pollutant combinations. Li et al. (2020) reported that dibutyl phthalate, a typical plasticizer, and PS MPs showed antagonistic effects on *Chlorella pyrenoidosa*. Huang et al. (2021) found that bromide flame retardant tetrabromobisphenol A in combination with polyethylene (PE) MPs exhibited synergistic effects on Caco-2 cells and intestinal microbiota.

Despite considerable reports studying the combined toxicity of MPs with different pollutants, research on their toxic mechanisms remains limited. Recently, You et al. (2021) demonstrated through metabolomics that interference with DNA synthesis is one of the combined toxic mechanisms of PS M/NPs and ciprofloxacin on Synechocystis sp. Ji et al. (2021a) revealed that the intracellular fate of PS-BaP complexes, such as their uptake, trafficking, and dissociation, critically influenced toxicity, with mechanisms linked to ROS generation and mitochondrial dysfunction. Although the interest in combined toxic effects of MPs and other environmental pollutants is growing, there is a lack of comprehensive data on polypropylene (PP) MPs, despite their high environmental relevance. PP plastic is currently the second most commonly used general-purpose plastic worldwide (Watanabe et al., 2018). Due to its relatively low heat resistance, poor resistance to ultraviolet radiation, and oxidation, it quickly ages, weathers, and decomposes into smaller MP particles during environmental transport. These particles accumulate in the ocean or spread widely through air transport, making PP one of the most serious plastic pollutants in aquatic environments (Yan et al., 2024). Currently, research on MPs has predominantly focused on PS and PE, while studies concerning PP are relatively scarce, and very few discussed its combined effects with PAHs. Romdhani et al. (2022) indicated that environmental MPs alone and mixed with BaP induced cytotoxic and genotoxic effects on hemocytes of *Mytilus galloprovincialis*. Cheng et al. (2024) found that polyethylene terephthalate (PET), PP MPs and absorbed BaP led to more DNA damage in microalgae, potentially causing additional disturbances in cellular energy metabolism compared to PET/PP MPs. However, further understanding of the combined toxicity mechanisms on mammalian cells such as mouse macrophage cell line RAW264.7, and the underlying molecular cascade linking initial oxidative damage to inflammatory responses and global proteomic alterations, remain unexplored. This gap hinders a mechanistic understanding pertinent to potential human health impacts.

Herein, to address the research gap mentioned, a study on the in vitro exposure of the very frequently found PP MPs, with notorious BaP was designed and conducted. We evaluated the combined toxicity of PP MPs and BaP on mouse macrophage cell line RAW264.7, comparing it with the individual toxicity of BaP. It was found that co-exposure to PP MPs and BaP significantly reduced cell viability, increased Lactate dehydrogenase (LDH) release and apoptosis. In addition, co-exposure led to heightened oxidative stress, including suppressed superoxide dismutase (SOD) and catalase (CAT) activities, reduced glutathione (GSH) levels, and increased malondialdehyde (MDA) and ROS levels. Furthermore, TMT proteomics technology elucidated differentially expressed proteins (DEPs) and affected signaling pathways in exposed cells, revealing that co-exposure induced more pronounced immune activation and inflammatory responses. It provided more clues for explaining the combined toxicity mechanisms of PP MPs and BaP co-exposure.

2. Materials and methods

2.1. Preparation of PP MPs

Common methods for preparing MPs simulants include purchasing commercial plastic nanoparticles (Trevisan et al., 2019), synthesizing monodisperse small-sized plastic particles through polymerization reactions (Wang et al., 2020), and grinding large plastic materials (Ateia et al., 2020). The nonsolvent induced phase separation (NIPS) method involves dissolving a polymer in a solvent to form a homogeneous solution, followed by the slow addition of a nonsolvent to induce phase separation and recrystallization of the polymer, this method is commonly used for preparing microporous membranes (Lu et al., 2017) and is favored for its simplicity, short processing time, and straightforward equipment requirements (Zhang et al., 2022). Based on previous research, PP MPs were prepared using NIPS method (Trevisan et al.,

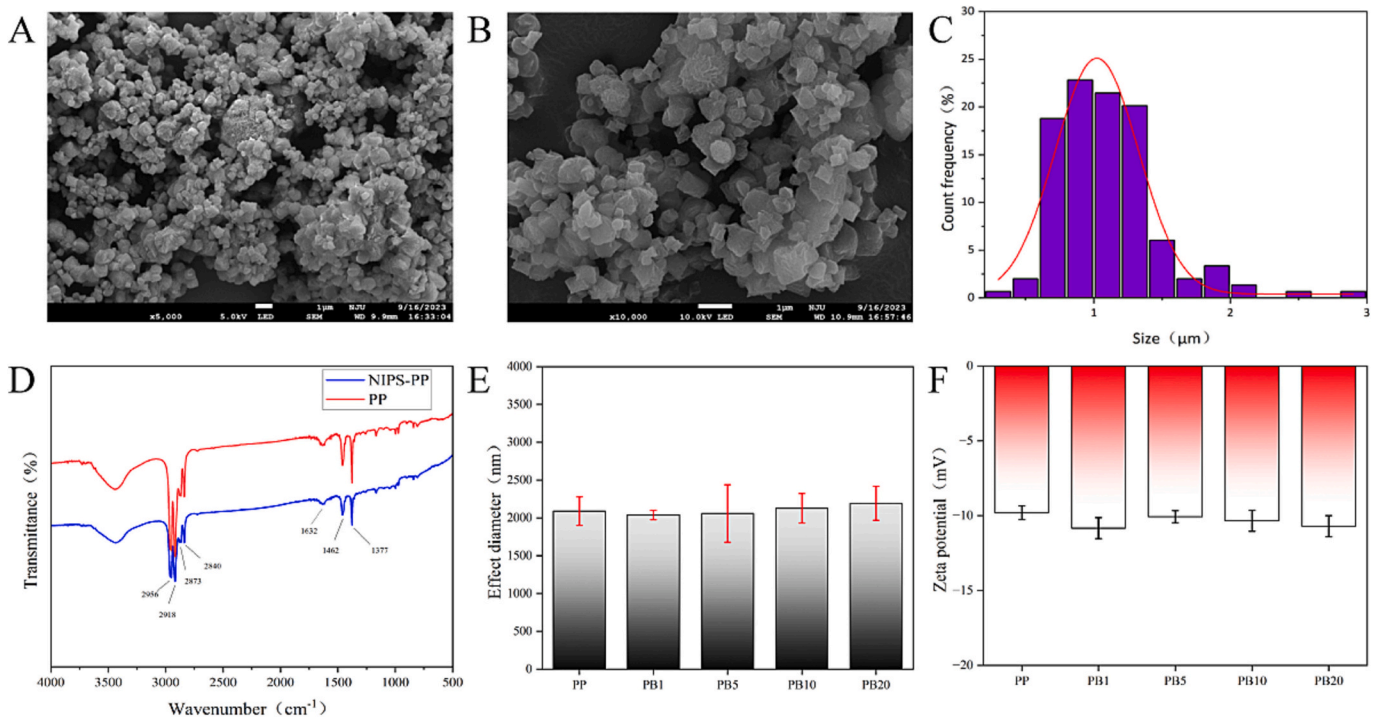

Fig. 1. SEM images of PP MPs prepared by the NIPS method (A: 5000 magnification; B: 10000 magnification; C: particle size distribution); Infrared spectra of PP MPs and original PP (D); Hydrodynamic dimensions (E) and zeta potentials (F) of PP and PP@BaP MPs dispersions.

2019). PP particles were purchased from Sigma-Aldrich (Shanghai, China). The specific steps are as follows: 1 g PP was placed into 50 mL of xylene, stirred and heated to 110 °C for 30 min, followed by adding 120 mL of ethanol. After cooling to room temperature, the suspension was filtered by vacuum filtration using polytetrafluoroethylene membrane. The solids were washed with ethanol three times, then collected, and dried in a vacuum drying oven at 60 °C for 24 h.

2.2. Preparation of PP@BaP MPs

During environmental transport, PAHs such as BaP readily adsorb onto MPs to form MP-pollutant complexes, enabling their co-dispersion (Bhagat et al., 2021). Therefore, to simulate this process, we prepared a composite mixture of PP MPs and BaP (PP@BaP MPs). According to previous studies, PP@BaP MPs was prepared as follows (Ji et al., 2021b): Firstly, PP MPs were dispersed in dimethyl sulfoxide (DMSO) to a concentration of 30 mg/mL, and BaP stock solution in DMSO was diluted with Dulbecco's modified eagle medium (DMEM) containing 10% fetal bovine serum (FBS) to 1–20 μM. Then, PP MPs suspension was added to the BaP solutions to achieve a final concentration of 100 μg/mL with BaP concentrations respectively at 1, 5, 10, and 20 μM in complete culture medium. Finally, these mixtures were incubated at 600 rpm at 37 °C for 24 h, and designated as Group PB (PB1, PB5, PB10, and PB20, respectively). The solutions of 1, 5, 10, and 20 μM BaP without PP MPs were designated as Group B (B1, B5, B10, and B20, respectively), and the suspension of PP MPs at 100 μg/mL was designated as Group PP.

2.3. Characterization of PP and PP@BaP MPs

The size and morphology of PP MPs were characterized by a scanning electron microscopy (SEM) (S-4800, Hitachi, Japan). The surface functional groups of PP MPs were analyzed by a Fourier transform infrared (ATR-FTIR) spectrometer (Nicolet iS10, ThermoFisher Scientific, USA). After ultrasonication in DMEM containing 0.5% DMSO for 10 min, the hydrodynamic size and zeta potential of PP@BaP MPs were measured by a dynamic light scattering (DLS) instrument (Brookhaven 90Plus) (Du et al., 2023).

2.4. Cell culture and in vitro exposure

RAW264.7 cells were cultured in high glucose DMEM, supplemented with 10% FBS and without penicillin/streptomycin. Cells were maintained in a CO_2 incubator at 37 °C with 5% CO_2. Passaging was performed when the cell growth reached 80% to 90% confluency. Cells then were stimulated with medium containing PP MPs, BaP and PP@BaP MPs dispersions respectively to investigate the individual and combined toxicity.

2.5. Cell viability assay

Cell viability of RAW264.7 cells after exposure to Groups PP, B and PB for 24/48 h was evaluated using the Cell Counting Kit-8 (CCK-8) (Beyotime, China) (Kong et al., 2021). Details are described in Supplementary Text S1.2.

2.6. LDH release measurement

LDH content in the culture medium of RAW264.7 cells after exposure to Groups PP, B and PB for 24/48 h was determined using the CheKine™ Micro Lactate Dehydrogenase (LDH) Assay Kit (Abbkine, China) (Chen et al., 2024a). Details are described in Supplementary Text S1.3.

2.7. Cell apoptosis assay

The apoptosis rate of RAW264.7 cells after exposure to Groups PP, B and PB for 24/48 h was analyzed using the Annexin V-FITC/PI Double Staining Apoptosis Detection Kit (Beyotime China) (Lei et al., 2022). Details are described in Supplementary Text S1.4.

2.8. Oxidative stress measurement

Intracellular ROS level, SOD activity, CAT activity, GSH content, and

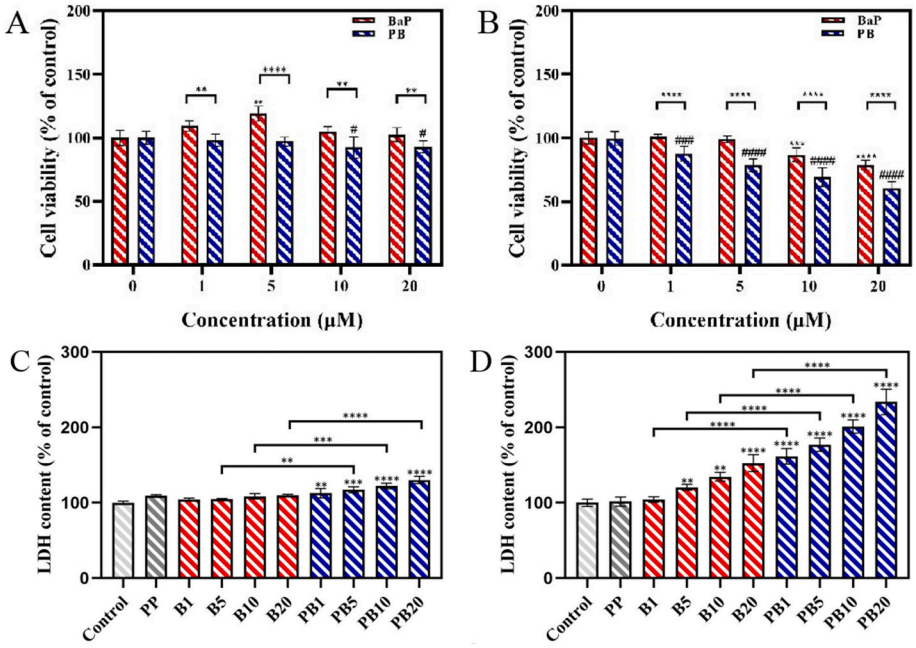

Fig. 2. Cell viability of RAW264.7 cells after exposure to BaP and PP@BaP MPs for 24 h (A) and 48 h (B); LDH content in the culture medium after exposure to BaP, PP and PP@Bap MPs for 24 h (C) and 48 h (D).

MDA content of RAW264.7 cells after exposure to Groups PP, B and PB for 24 h were assessed using corresponding detection kits. Details are described in Supplementary Text S1.5–1.9.

2.9. Proteomics

Protein lysate samples from the Groups B20 and PB20, which exhibited the most significant toxicity, were analyzed using TMT-10 labeling reagents (Mertins et al., 2018). A control group (Group C) with no stimulant addition was included, with each group having three replicates. Protein extraction and protein concentration determination using the BCA Protein Assay Kit were conducted. The experimental workflow included trypsin digestion, peptide labeling, reverse-phase liquid chromatography separation, and mass spectrometry analysis. Details are described in Supplementary Text S1.10.

2.10. IL-6 protein level assay

The concentration of Interleukin-6 (IL-6) in the culture medium of RAW264.7 cells after exposure to Groups PP, B and PB for 24 h was determined by enzyme-linked immunosorbent assay (ELISA) using the Mouse IL-6 ELISA Kit (Excell China) (Teng et al., 2019). Details are described in Supplementary Text S1.11.

2.11. Data analysis

Data analysis was conducted using Microsoft Office Excel 2020 software. The results were expressed as mean ± standard deviations (SD). All the measurements were repeated at least twice, with at least three replicates per group. Differences between any two time points or between two groups at the same time point are analyzed using One-way ANOVA, where * $p < 0.05$, ** $p < 0.01$, *** $p < 0.001$, **** $p < 0.0001$. The mass spectrometry data in proteomics were analyzed using a Proteome Discoverer 2.4.1.15 (ThermoFisher Scientific). Details are described in Supplementary Text S1.10.

3. Results and discussion

3.1. Characterization of MPs

The surface morphology of PP MPs was observed via SEM, as shown in Fig. 1A-B. The prepared PP MPs exhibited irregular shapes and rough surfaces, with some particles showing filamentous structures and gaps on the surface. Size analysis of the particles (Fig. 1C) indicated that the average size of PP MPs is 1.10 μm, with the majority of particles distributed between 0.9 and 1.5 μm, accounting for over 80% of the total quantity.

The surface functional groups of PP MPs were characterized by ATR-FTIR, as shown in Fig. 1D. The spectrum of PP MPs is in good agreement with that of the original PP, with no other absorption peaks observed, indicating that the surface chemical properties of PP did not change during preparation.

The hydrodynamic size and zeta potential of PP and PP@BaP MPs were determined, as shown in Fig. 1E-F. In dispersion, the hydrodynamic size of PP MPs (Fig. 1E) is slightly larger than that observed by SEM, indicating non-uniform particle size and lack of monodispersed in DMEM containing 0.5% DMSO. The coexistence of BaP has no visible effect on the hydration diameter. The zeta potential of PP MPs dispersion is approximately −10 mV, as shown in Fig. 1F, with no various change after the coexistence of BaP. These results suggest that PP MPs have a certain degree of aggregation in the dispersion, and the presence of BaP does not apparently affect their aggregation state.

3.2. Cytotoxicity of PP@BaP MPs compared to BaP alone

Before investigating the combined system of BaP and PP MPs, we first explored the toxic effects of PP MPs individually on RAW264.7 cells, as illustrated in Fig. S1. It is evident that PP MPs at concentrations of 50–150 μg/mL did not cause obvious changes in cell viability after 24 or 48 h of exposure compared to the control group. This indicated that PP MPs exhibited very low toxicity to RAW264.7 cells within this concentration range. Therefore, in subsequent experiments, we used the PP MPs dispersion at a concentration of 100 μg/mL as representative to maintain a consistent microplastic influence.

The toxicity difference between the exposure of BaP and PP@BaP

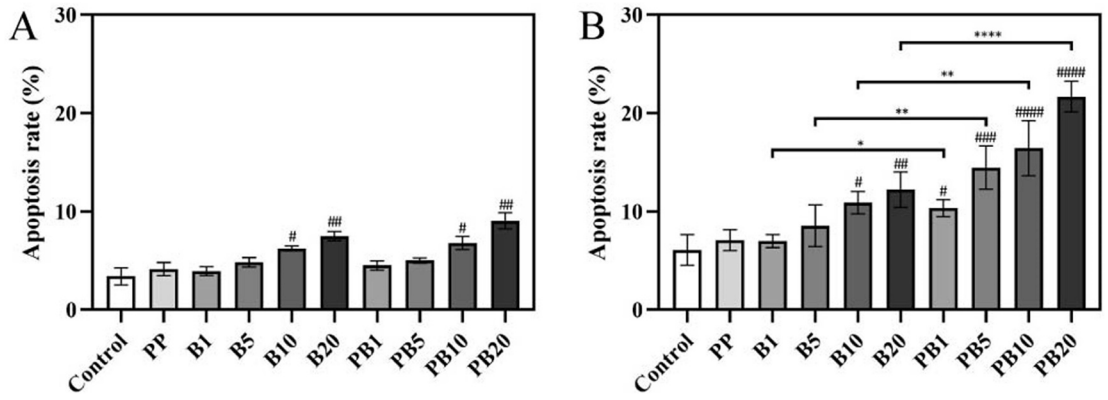

Fig. 3. Apoptosis rates of RAW264.7 cells after exposure to BaP, PP and PP@BaP MPs for 24 h (A) and 48 h (B).

MPs to RAW264.7 cells were compared, as shown in Fig. 2A-B. During stimulation for 24 h, as concentration of BaP rose from 0 to 1 μM and then to 5 μM, cell viability gradually increased to approximately 110% and then to 120% relative to control group. However, as the concentration of BaP further increased, cell viability began to decline, eventually reaching around 90%, showing no significant difference from the control group. Although PP@BaP MPs did not apparently inhibit cell viability, it showed significant differences compared to individual BaP. After longer exposure of 48 h, BaP at concentrations of 1–5 μM did not obviously affect RAW264.7 cells, with cell viability remaining above 90%. However, when the concentration increased to 10–20 μM, cell viability significantly decreased in a dose-dependent manner. These results suggest that under short-term, low-concentration exposure, BaP promotes the proliferation of RAW264.7 cells, possibly as a cellular response to adapt to external stress. However, when the exposure time is prolonged and the concentration of BaP is increased, the stress from the external stimulus exceeds the cells' adaptive capacity, leading to an enhanced cytotoxicity. Regardless of comparison with control or BaP alone, combined exposure led to a significant decrease in cell viability.

Cell membrane damage was evaluated by measuring the release of LDH, as shown in Fig. 2C-D. Whether at 24 or 48 h, PP MPs alone showed no obvious changes compared to the control group. Similar to cell viability results, after 24 h stimulation, BaP did not induce apparent increase in LDH level, while PP@BaP MPs led to an increase in LDH release. After 48 h, high concentrations of BaP resulted in approximately a 50% increase in LDH release, while PP@BaP MPs induced a maximum increase of about 130%, significantly higher than that induced by sole BaP stimulation. Cell membrane damage may result from BaP stimulation or the interaction of MPs with the cell membrane. Choi et al. (2021) reported severe hemolysis of red blood cells exposed to 1 mg/mL PE particles, possibly due to the sharp edges or specific shapes of PE particles damaging the red blood cell membrane.

The effects of PP MPs, BaP and PP@BaP MPs on the apoptosis rate of RAW264.7 cells were investigated, as shown in Fig. 3. Similar to the results above, whether at 24 or 48 h, PP MPs alone showed no obvious changes compared to the control group. After 24 h stimulation, the apoptosis rate showed a concentration-dependent increase with BaP, with no obvious difference between Group B and PB. When extending the stimulation time to 48 h, the apoptosis rate was induced by BaP increased, but significant differences from Group C were observed only

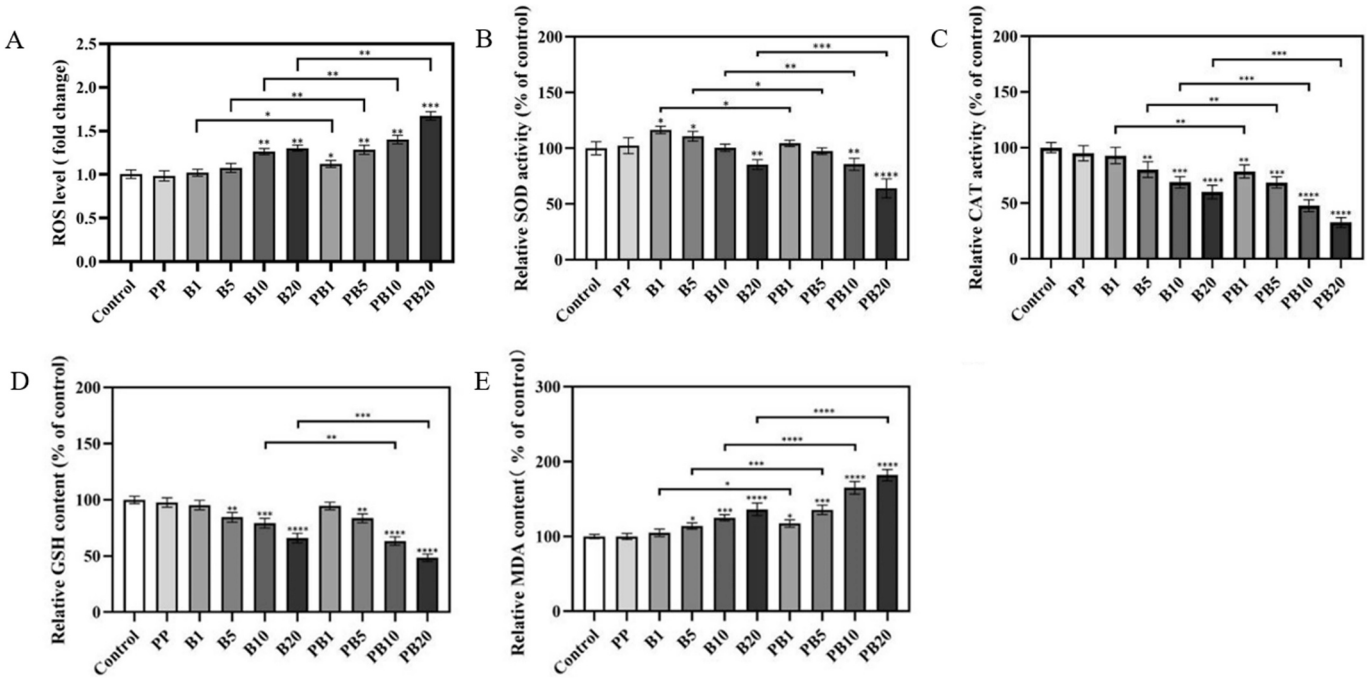

Fig. 4. Intracellular ROS levels (A), SOD activity (B), CAT activity (C), GSH content (D) and MDA content (E) in RAW264.7 cells after exposure to BaP, PP and PP@BaP MPs for 24 h.

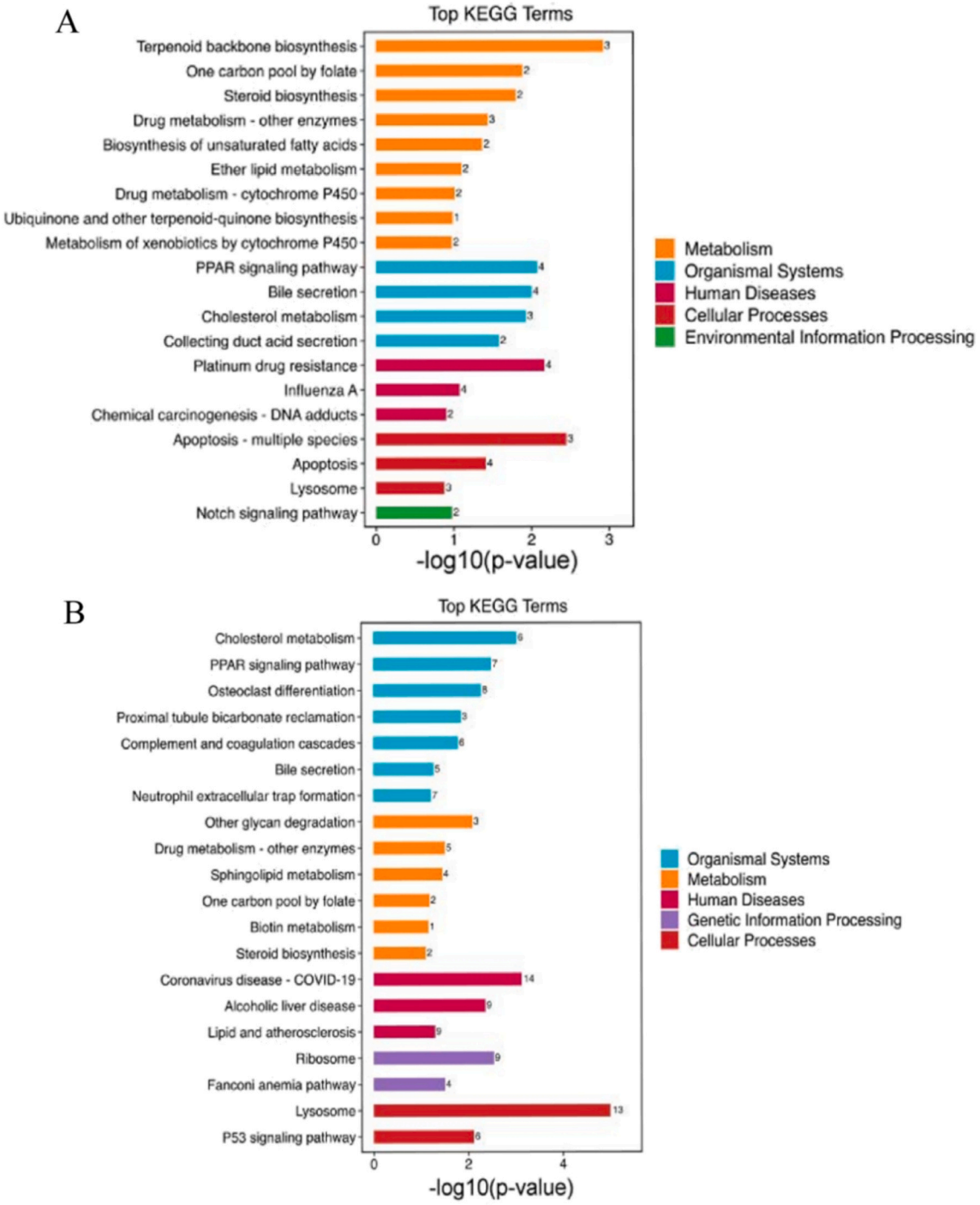

Fig. 5. KEGG pathway enriched by DEPs in RAW264.7 cells affected by B20 (A) and PB20 (B). The number on the bar is the number of differentially expressed proteins annotated to the pathway, and different colors of the bar represent different KEGG Level information.

at higher concentrations. However, PP@BaP MPs induced higher cell apoptosis at the same concentration, showing significant differences.

Based on the results of cell viability, LDH release, and apoptosis assays mentioned above, it was found that under high concentration and long-time stimulation, BaP exhibited toxicity to RAW264.7 cells. Additionally, PP MPs alone showed no obvious toxic effects on the cells, while the combined exposure of PP MPs with BaP exacerbated the BaP cytotoxicity. Previous studies have indicated that environmental pollutants, when combined with fine particulate matters, could exert combined toxic effects (Ji et al., 2021b; Wang and Wang, 2018). Besides, toxicity of PP@BaP MPs was greater than the sum of the toxicities of PP MPs alone and BaP alone after 48 h, indicating a clear synergistic effect between PP MPs and BaP further increasing the toxicity to cells. These damages destructed the integrity of the cell membrane, leading to increased cell apoptosis and consequently reducing cell viability, and therefore confirming the interactive effects hypothesized for MP-pollutant complexes.

3.3. *Oxidative stress of PP@BaP MPs compared to BaP alone*

The intracelluar ROS levels affected by BaP and PP@BaP MPs were measured, with results presented as fold changes in DCFH-DA

fluorescence intensity, as shown in Fig. 4A. Similar to the results above, PP MPs alone showed no obvious changes compared to the control group. The results indicated that even at low concentrations, co-exposure of PP MPs and BaP can induce increased intracellular ROS levels. Moreover, after the exposure of PP@BaP MPs, there was apparent elevation in intracellular ROS levels. Meanwhile, there was a significant difference between the intracellular ROS levels after stimulation with BaP and PP@BaP MPs. Earlier research has also shown that RAW264.7 macrophages could engulf exogenous stimuli, subsequently generating large amounts of ROS and triggering the release of inflammatory factors, ultimately leading to cell damage or apoptosis (Xu et al., 2018). In this study, however, we did not observe apparent changes in side scatter, suggesting that cellular phagocytosis of the MP particles might be weak. This contrasted with findings from some studies where cells were observed to engulf particulate matters (Chen et al., 2024b). Nevertheless, PP MPs still induced strong oxidative stress, implying that the interaction between microplastics and pollutants may alter their respective bio-reactivities. From Fig. 4B, PP@BaP MPs stimulation significantly decreased SOD activity compared to BaP stimulation alone. As shown in Fig. 4C, CAT activity decreased gradually with the BaP concentration increased. Co-exposure of PP MPs and BaP led to a greater decrease in cellular CAT activity. From Fig. 4D, the GSH content in RAW264.7 cells significantly decreased after stimulation with PP@BaP MPs. Finally, from Fig. 4E, as the concentration of BaP increased, MDA content of RAW264.7 cells gradually increased. PP@BaP MPs further increased MDA content showing a significant difference compared to BaP alone.

Summarizing the above results, we easily observed that BaP induced oxidative stress in RAW264.7 cells, with a certain concentration dependency. PP MPs alone did not exert obvious effect on cellular oxidative stress, while BaP showed notable oxidative stress. Moreover, combined exposure to PP MPs and BaP resulted in a significantly trigger oxidative stress response, further inhibiting the activity of oxidative stress enzymes, reducing the levels of antioxidants, and promoting the accumulation of oxidative stress products, which finally led to severer oxidative damage to cells. Such strong oxidative stress exceeded the cells' own ability to resist oxidative stress, resulting in a large amount of cell apoptosis, and ultimately manifested as a significant decrease in cell viability. This systematic dysregulation of the antioxidant defense system (SOD, CAT, GSH) coupled with elevated peroxidation (MDA) provided a mechanistic explanation for the synergistic cytotoxicity, addressing the specific gap in oxidative stress profiling for this pollutant combination. The pattern was consistent with, yet more comprehensive than, reports of ROS/MDA increased in microalgae exposed to similar mixtures (Cheng et al., 2024).

3.4. Potential pathways affected by the co-exposure of PP MPs and BaP

Based on the above results, we found that PP MPs alone did not cause obvious cytotoxicity or induce notable oxidative stress in cells. However, PP@BaP MPs, compared to individual BaP, induced a significant increase or enhancement in cellular toxicity and elevated levels of oxidative stress. In order to unravel the mechanisms underlying the difference in cellular toxicity of PP@BaP MPs and BaP, we conducted a proteomic analysis on stimulated RAW264.7 cells. According to TMT quantitative proteomics, a total of 7319 proteins were identified. Among these proteins, 138 and 344 DEPs were selected in Group B20 and Group PB20, respectively (the details of the DEPs are listed in Tables S1–2). As shown in Fig. S1–2, GO annotations of these DEPs were analyzed. Group B20 significantly enriched proteins related to the metabolism of substances such as cholesterol and lipids, protein ubiquitination, cell proliferation and apoptosis, and oxidative stress response. Meanwhile, Group PB20 significantly enriched proteins associated with cell division, chemokine and cytokine production, endocytosis, and cell apoptosis. Additionally, compared to individual exposure to BaP, co-exposure obviously influenced proteins involved in immune responses, inflammatory responses, and cell differentiation. It is noteworthy that proteins associated with cytokine production (e.g. CCL5, IL1B) and immune response (e.g. TLR4, NF-κB) were enriched in the co-exposure group, indicating that PP-MPs combined with BaP triggered a more severe immune stress. This finding may explain the origin of their synergistic toxicity. Previous studies have reported that RAW264.7 cells could differentiate into anti-inflammatory macrophages under the influence of ROS and pro-inflammatory cytokines after mono-2-ethylhexylphthalate stimulation (Bølling et al., 2012). The results in our study indicated that both BaP and PP@BaP MPs affected cell proliferation and apoptosis. However, co-exposure induced immune stress more rapidly and significantly, resulting in lower cell viability.

Meanwhile, the KEGG pathways enriched by DEPs in RAW264.7 cells affected by Group B20 and PB20 were analyzed, as shown in Fig. 5A-B. A comparison of the experimental Groups B20 and PB20 revealed significant enrichment in both the “PPAR signaling pathway” and “Lysosome” signal pathways. Peroxisome proliferator-activated receptors (PPARs) act as ligand-activated transcription factors regulating gene expression, participating in glucose and lipid metabolism as well as immune regulation (Montaigne et al., 2021). Lysosomes, highly conserved organelles in eukaryotic cells, are traditionally involved in the degradation of various biomacromolecules, including proteins, nucleic acids, and polysaccharides, and are associated with cellular autophagy. Recent studies have shown that lysosomes also serve as a convergence center for multiple core cellular signaling pathways (such as mTORC1, AMPK, JAK2-STAT3), playing important roles in nutrient sensing, cell growth, energy metabolism, immune response, and aging processes (Yang and Wang, 2021; Zhang et al., 2014). In co-exposure group, lysosomal pathway disruption likely compromised organelle function, thereby worsening autophagy impairment and oxidative stress. Furthermore, apparent differences were observed in the “PPAR signaling pathway” and “lysosome” signal pathways between Group B20 and Group PB20. This indicated that both individual BaP and PP@BaP MPs significantly affected the proliferation, autophagy apoptosis, and immune response processes in RAW264.7 cells. However, the impact of PP@BaP MPs was more profound, consistent with the cytotoxicity results. This finding aligned with our previous observations regarding ROS/MDA levels. DEPs in Group PB20 were also significantly enriched in signaling pathways related to inflammation and immune response, such as the “Toll-like receptor signaling pathway”, “Neutrophil extracellular trap formation” and “IL-17 signaling pathway.”, further indicating that cells in Group PB20 exhibited a more intense inflammatory response.

The proteomic results herein fill a critical gap in the systematic understanding of the molecular pathways perturbed by this co-exposure. Crucially, these findings revealed a pronounced activation of immune-inflammatory pathways in the combined toxicity of PP@BaP MPs. While exposure to BaP alone elicited a stress-response profile dominated by metabolism and apoptosis, the co-exposure group exhibited a distinct shift towards an inflammatory phenotype. In a study on rat liver tissue, it was found that the combined exposure to MPs and BaP led to the lowest expression of Nrf2 and the highest expression of P38, NF-κB and TNF-α, suggesting that the introduction of MPs caused a more significant inflammatory response in cells (Li et al., 2024). Supported by the above report, our research exposited that PP MPs not only exacerbated the toxicity of BaP but also qualitatively altered cellular response, likely by providing a persistent immunostimulatory signal synergized with oxidative stress, thereby elucidating the mechanism underlying the composite toxicity.

3.5. Analysis of IL-6 protein expression

As an important inflammatory mediator, IL-6 plays a key role in the inflammatory response. It can induce the recruitment and activation of inflammatory cells, promote the release of inflammatory factors and the occurrence of inflammatory reactions (Jürgen et al., 2011). As discussed in the previous section, we inferred that co-exposure of PP MPs and BaP

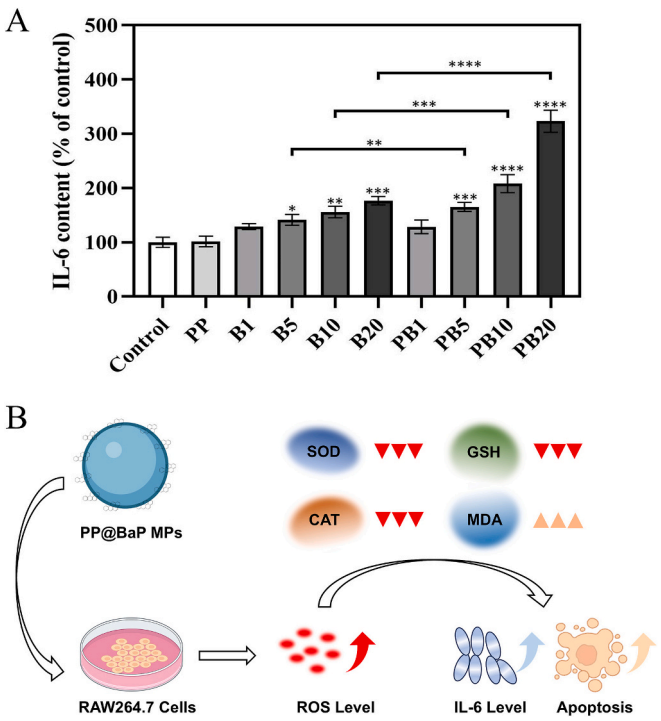

Fig. 6. IL-6 levels in culture medium of RAW264.7 cells after exposure to BaP, PP and PP@BaP MPs for 24 h (A). Schematic diagram of PP@BaP MPs-induced oxidative damage and inflammatory response in RAW264.7 cells (B).

might trigger a more serious inflammatory response in RAW264.7 cells. Hereinafter, this speculation was verified by determining the expression of IL-6 protein in cells using the ELISA method. The results were shown in Fig. 6A. We observed that PP MPs did not apparently affect IL-6 protein expression in RAW264.7 cells. BaP stimulation led to an up-regulation of IL-6 protein expression in RAW264.7 cells in a concentration-dependent manner, indicating a gradual and intense inflammatory response. Co-exposure of PP MPs and BaP resulted in a significant increase in the expression of the IL-6 protein, indicating that a more intense inflammatory response occurred in the cells. This was also in the same trend as the results of cell viability, indicating that the inflammatory response may be one of the important reasons for the deteriorated state of RAW264.7 cells in the co-exposure group.

This result provided direct evidence for the inflammatory pathway activation indicated by proteomics. Integrated with the observed systematic oxidative damage, it demonstrated that co-exposure to PP MPs and BaP synergistically drove greater cytotoxicity by inducing significant oxidative injury and triggering a specific inflammatory signaling network (Fig. 6B). Thereby, the findings in this work systematically buckled up the systematically elucidated mechanistic chain from oxidative stress to inflammatory activation.

4. Conclusions

In this study, we investigated the synergistic toxicity of combined stimulation of NIPS-prepared PP MPs and BaP on RAW264.7 cells. While PP MPs alone exhibited negligible effects, co-exposure to BaP and PP MPs significantly reduced cell viability, increased LDH release, and elevated apoptosis compared to exposure to either BaP or PP MPs alone. Moreover, co-exposure led to heightened oxidative stress, characterized by suppressed SOD and CAT activities, reduced GSH levels, and increased MDA and ROS levels. The toxicity and oxidative stress of PP@BaP MPs was greater than the sum of PP MPs alone and BaP alone, demonstrating a synergistic or enhanced effect between PP MPs and BaP. More importantly, proteomics revealed that co-exposure uniquely triggered pronounced activation of immune-inflammatory pathways, validated by the IL-6 upregulation. The intracellular interactions and migration behaviors of BaP and PP MPs require further investigation to fully understand their mechanisms of action. As the first attempt to conduct toxicoproteomic investigation on this environmentally relevant combination, this work not only bridges a critical knowledge gap but also provides a molecular framework for assessing the combined risks of MPs and co-pollutants.

CRediT authorship contribution statement

Ye-xuan Zhang: Writing – original draft, Visualization, Methodology, Formal analysis. **Rui Hou:** Writing – original draft, Investigation, Formal analysis, Data curation. **Si-si Chen:** Visualization, Methodology, Formal analysis. **Xue-wen Guo:** Software, Data curation. **Hong-juan Chen:** Methodology, Formal analysis. **Li Mao:** Resources, Funding acquisition. **Wei-juan Zheng:** Resources, Investigation. **Hong-zhen Lian:** Writing – review & editing, Project administration, Methodology, Funding acquisition, Conceptualization.

Declaration of competing interest

The authors declare that they have no known competing financial interests or personal relationships that could have appeared to influence the work reported in this paper.

Acknowledgments

This work was supported by the National Natural Science Foundation of China (22176085, 21874065, 91643105).

Appendix A. Supplementary data

Supplementary data to this article can be found online at https://doi.org/10.1016/j.scitotenv.2026.181707.

Data availability

Data will be made available on request.

References

Ateia, M., Zheng, T., Calace, S., Tharayil, N., Pilla, S., Karanfil, T., 2020. Sorption behavior of real microplastics (MPs): insights for organic micropollutants adsorption on a large set of well-characterized MPs. Sci. Total Environ. 720, 137634.
Bhagat, J., Nishimura, N., Shimada, Y., 2021. Toxicological interactions of microplastics (nanoplastics) and environmental contaminants: current knowledge and future perspectives. J. Hazard. Mater. 405, 123913.
Bølling, A.K., Ovrevik, J., Samuelsen, J.T., Holme, J.A., Rakkestad, K.E., Mathisen, G.H., et al., 2012. Mono-2-ethylhexylphthalate (MEHP) induces TNF-α release and macrophage differentiation through different signalling pathways in RAW264.7 cells. Toxicol. Lett. 209, 43–50.
Chen, S., Xie, D.F., Li, S.Y., Luo, J.H., Han, Y., Guo, H.J., et al., 2024a. TAB182 regulates glycolytic metabolism by controlling LDHA transcription to impact tumor radiosensitivity. Cell Death Dis. 15, 209.
Chen, S., Zhang, Y.X., Chen, H.J., Zheng, W.J., Hu, X., Mao, L., et al., 2024b. Surface property and in vitro toxicity effect of insoluble particles given by protein corona: Implication for PM cytotoxicity assessment. Eco-Environ. Health 3, 137–144.
Cheng, S., Keang, K., Cross, J.S., 2024. Evidence that microplastics at environmentally relevant concentration and size interfere with energy metabolism of microalgal community. J. Hazard. Mater. 476, 134995.
Choi, D., Hwang, J., Bang, J., Han, S., Kim, T., Oh, Y., et al., 2021. In vitro toxicity from a physical perspective of polyethylene microplastics based on statistical curvature change analysis. Sci. Total Environ. 752, 142242.
Çobanoğlu, H., Belivermiş, M., Sıkdokur, E., Kılıç, O., Çayır, A., 2021. Genotoxic and cytotoxic effects of polyethylene microplastics on human peripheral blood lymphocytes. Chemosphere 272, 129805.
Dang, F., Wang, Q.Y., Huang, Y.N., Wang, Y.J., Xing, B.S., 2022. Key knowledge gaps for one health approach to mitigate nanoplastic risks. Eco-Environment & Health 1, 11–22.
Du, T.T., Yu, X., Song, S., Li, T., Xu, S.M., Wu, L.J., 2023. Aging of nanoplastics significantly affects protein corona composition thus enhancing macrophage uptake. Environ. Sci. Technol. 57, 3206–3217.

Feng, Y.D., Tu, C., Li, R.J., Wu, D., Yang, J., Xia, Y.K., et al., 2023. A systematic review of the impacts of exposure to micro- and nano-plastics on human tissue accumulation and health. Eco-Environ. Health 2, 195–207.
Gewert, B., Plassmann, M.M., Macleod, M., 2015. Pathways for degradation of plastic polymers floating in the marine environment. Environ Sci Process Impacts 17, 1513–1521.
Goswami, P., Ohura, T., Subasinghe, S., Wickrama-Arachchige, A., Takeuchi, S., Imaki, M., et al., 2023. Voyaging of halogenated polycyclic aromatic hydrocarbons, an emerging group of pollutants, on micro-mesoplastics in the marine environment. J. Hazard. Mater. 460, 132502.
Hartmann, N.B., Hüffer, T., Thompson, R.C., Hassellöv, M., Verschoor, A., Daugaard, A. E., et al., 2019. Are we speaking the same language? Recommendations for a definition and categorization framework for plastic debris. Environ. Sci. Technol. 53, 1039–1047.
Hirt, N., Body-Malapel, M., 2020. Immunotoxicity and intestinal effects of nano- and microplastics: a review of the literature. Part. Fibre Toxicol. 17, 57.
Huang, W., Yin, H., Yang, Y., Jin, L., Lu, G., Dang, Z., 2021. Influence of the co-exposure of microplastics and tetrabromobisphenol a on human gut: simulation in vitro with human cell Caco-2 and gut microbiota. Sci. Total Environ. 778, 146264.
IARC Working Group on the Evaluation of Carcinogenic Risks to Humans, 2010. Some non-heterocyclic polycyclic aromatic hydrocarbons and some related exposures. IARC Monogr. Eval. Carcinog. Risks Hum. 92, 1–853.
Ji, Y.X., Wang, Y.Q., Shen, D.Z., Kang, Q., Chen, L.X., 2021b. Mucin corona delays intracellular trafficking and alleviates cytotoxicity of nanoplastic-benzopyrene combined contaminant. J. Hazard. Mater. 406, 124306.
Ji, Y.X., Wang, Y.Q., Shen, D.Z., Kang, Q., Ma, J.P., Chen, L.X., 2021a. Revisiting the cellular toxicity of benzo[a]pyrene from the view of nanoclusters: size- and nanoplastic adsorption-dependent bioavailability. Nanoscale 13, 1016–1028.
Jürgen, S., Athena, C., Dirk, S., Stefan, R., 2011. The pro- and anti-inflammatory properties of the cytokine interleukin-6. Biochim. Biophys. Acta-Mol. Cell Res. 1813, 878–888.
Kershaw, P.J., Rochman, C.M., 2016. Sources, Fate and Effects of Microplastics in the Marine Environment: Part Two of a Global Assessment. International Maritime Organization, London.
Kong, L., Wu, Y.X., Li, C., Liu, J., Jia, J.B., Zhou, H.Y., et al., 2021. Nano-cell and nano-pollutant interactions constitute key elements in nanoparticle-pollutant combined cytotoxicity. J. Hazard. Mater. 418, 126259.
Kongpran, J., Kliengchuay, W., Niampradit, S., Sahanavin, N., Siriratruengsuk, W., Tantrakarnapa, K., 2021. The health risks of airborne polycyclic aromatic hydrocarbons (PAHs): upper North Thailand. GeoHealth 5, e2020GH000352.
Lechner, A., Ramler, D., 2015. The discharge of certain amounts of industrial microplastic from a production plant into the river Danube is permitted by the Austrian legislation. Environ. Pollut. 200, 159–160.
Lei, S., Zhang, J., Blum, N.T., Li, M., Zhang, D.Y., Yin, W.M., et al., 2022. In vivo three-dimensional multispectral photoacoustic imaging of dual enzyme-driven cyclic cascade reaction for tumor catalytic therapy. Nat. Commun. 13, 1298.
Li, J., Liu, H., Chen, J.P., 2018. Microplastics in freshwater systems: a review on occurrence, environmental effects, and methods for microplastics detection. Water Res. 137, 362–374.
Li, S.L., Qiao, Z.P., Huang, M.D., Lao, Q.F., Zhang, Q.Q., Xing, Y., et al., 2024. Combined exposure of polystyrene microplastics and benzo[a]pyrene in rat: study of the oxidative stress effects in the liver. Ecotoxicol. Environ. Saf. 278, 116390.
Li, Z., Yi, X., Zhou, H., Chi, T., Li, W., Yan, K., 2020. Combined effect of polystyrene microplastics and dibutyl phthalate on the microalgae Chlorella pyrenoidosa. Environ. Pollut. 257, 113604.
Liu, L.J., Sun, Y.Z., Du, S.T., Li, Y.M., Wang, J., 2024. Nanoplastics promote the dissemination of antibiotic resistance genes and diversify their bacterial hosts in soil. Eco-Environ. Health 3, 1–10.
Lu, W., Yuan, Z., Zhao, Y., Zhang, H., Zhang, H., Li, X., 2017. Porous membranes in secondary battery technologies. Chem. Soc. Rev. 46, 2199–2236.
Mertins, P., Tang, L.C., Krug, K., Clark, D.J., Gritsenko, M.A., Chen, L.J., et al., 2018. Reproducible workflow for multiplexed deep-scale proteome and phosphoproteome analysis of tumor tissues by liquid chromatography-mass spectrometry. Nat. Protoc. 13, 1632–1661.
Montaigne, D., Butruille, L., Staels, B., 2021. PPAR control of metabolism and cardiovascular functions. Nat. Rev. Cardiol. 18, 809–823.
Palaniappan, S., Sadacharan, C.M., Rostama, B., 2021. Polystyrene and polyethylene microplastics decrease cell viability and dysregulate inflammatory and oxidative stress markers of MDCK and L929 cells in vitro. Expo. Health 14, 1–11.
Prata, J.C., da Costa, J.P., Girão, A.V., Lopes, I., Duarte, A.C., Rocha-Santos, T., 2019. Identifying a quick and efficient method of removing organic matter without damaging microplastic samples. Sci. Total Environ. 686, 131–139.
Romdhani, I., De Marco, G., Cappello, T., Ibala, S., Zitouni, N., Boughattas, I., et al., 2022. Impact of environmental microplastics alone and mixed with benzo[a]pyrene on cellular and molecular responses of Mytilus galloprovincialis. J. Hazard. Mater. 435, 128952.
Salimi, A., Alavehzadeh, A., Ramezani, M., Pourahmad, J., 2022. Differences in sensitivity of human lymphocytes and fish lymphocytes to polyvinyl chloride microplastic toxicity. Toxicol. Ind. Health 38, 100–111.
Teng, J., Huang, L.Z., Zhang, L.T., Li, J., Bai, H.L., Li, Y., et al., 2019. High-sensitive immunosensing of protein biomarker based on interfacial recognition-induced homogeneous exponential transcription. Anal. Chim. Acta 1067, 107–114.
Trevisan, R., Voy, C., Chen, S., Chen, S., Di Giulio, R.T., 2019. Nanoplastics decrease the toxicity of a complex PAH mixture but impair mitochondrial energy production in developing zebrafish. Environ. Sci. Technol. 53, 8405–8415.
Wang, Q., Bai, J., Ning, B., Fan, L., Sun, T., Fang, Y., et al., 2020. Effects of bisphenol a and nanoscale and microscale polystyrene plastic exposure on particle uptake and toxicity in human Caco-2 cells. Chemosphere 254, 126788.
Wang, W., Wang, J., 2018. Different partition of polycyclic aromatic hydrocarbon on environmental particulates in freshwater: microplastics in comparison to natural sediment. Ecotoxicol. Environ. Saf. 147, 648–655.
Watanabe, R., Hagihara, H., Sato, H., 2018. Structure-property relationships of polypropylene-based nanocomposites obtained by dispersing mesoporous silica into hydroxyl-functionalized polypropylene. Part 1: toughness, stiffness and transparency. Polym. J. 50, 1057–1065.
Xia, C.L., Cai, L.P., Lam, S.S., Sonne, C., 2023. Microplastics pollution: economic loss and actions needed. Eco-Environment & Health 2, 41–42.
Xia, T., Kovochich, M., Nel, A.E., 2007. Impairment of mitochondrial function by particulate matter (PM) and their toxic components: implications for PM-induced cardiovascular and lung disease. Front. Biosci.-Landmark 12, 1238–1246.
Xu, F., Qiu, X., Hu, X., Shang, Y., Pardo, M., Fang, Y., et al., 2018. Effects on IL-1β signaling activation induced by water and organic extracts of fine particulate matter (PM2.5) in vitro. Environ. Pollut. 237, 592–600.
Xu, Y., Zhu, J., Hu, J., Zhang, Z., Li, L., Wu, Q., 2020. Co-exposure to different sized polystyrene microplastics and benzo[a]pyrene affected inflammation in zebrafish and bronchial-associated cells. Chin. Sci. Bull. 65, 4281–4890.
Yan, L., Yao, X., Wang, P., Zhao, C., Zhang, B., Qiu, L., 2024. Effect of polypropylene microplastics on virus resistance in spotted sea bass (Lateolabrax maculatus). Environ. Pollut. 342, 123054.
Yang, C., Wang, X., 2021. Lysosome biogenesis: regulation and functions. J. Cell Biol. 220, e202102001.
You, X., Cao, X., Zhang, X., Gao, J., Sun, W., 2021. Unraveling individual and combined toxicity of nano/microplastics and ciprofloxacin to Synechocystis sp. at the cellular and molecular levels. Environ. Int. 157, 106842.
Yu, S.J., Tan, Z.Q., Lai, Y.J., Li, Q.C., Liu, J.F., 2023. Nanoparticulate pollutants in the environment: analytical methods, formation, and transformation. Eco-Environ. Health 2, 61–73.
Zhang, C.S., Jiang, B., Li, M., Zhu, M., Peng, Y., Zhang, Y.L., 2014. The lysosomal v-ATPase-regulator complex is a common activator for AMPK and mTORC1, acting as a switch between catabolism and anabolism. Cell Metab. 20, 526–540.
Zhang, T.Q., Jia, Z.Q., Peng, W.J., Li, S.D., Wen, J.P., 2022. Preparation of 4-methyl-1-pentene membranes via non-solvent induced phase separation (NIPS). Eur. Polym. J. 178, 111480.
Zhong, H., Wu, M.J., Sonne, C., Lam, S.S., Kwong, R.W.M., Jiang, Y.L., et al., 2023. The hidden risk of microplastic-associated pathogens in aquatic environments. Eco-Environ. Health 2, 142–151.